

AN APPARATUS FOR EVALUATING LIQUID FIRE SUPPRESSANTS*

J.C. Yang, M.K. Donnelly, N.C. Privé, and W.L. Grosshandler
Building and Fire Research Laboratory
National Institute of Standards and Technology
Gaithersburg, MD 20899 USA

INTRODUCTION

Cup burners have been extensively used as a fire suppression efficiency screening tool for gaseous halon alternatives (e.g., [1]). In the search for alternatives to halons in fire suppression, it is likely that several types of condensed-phase compounds will be identified that may be delivered in droplet or aerosol form. Although cup burners have been used for evaluating condensed-phase agents (e.g., sodium bicarbonate powder), currently there is no apparatus designed specifically for screening liquid agents under well-controlled experimental conditions. The objective of this work is to design, construct, and demonstrate a bench-scale device capable of screening the fire suppression efficiency of liquid agents. The design of the apparatus is based on a well-characterized flame, a means to facilitate the introduction of liquid agents, and a way to generate liquid droplets. These individual components will be described in detail in the following sections. Since the project is on-going, its current status will be discussed, and some encouraging preliminary results will be presented.

In our liquid agent screening apparatus, we make use of a counterflow diffusion flame. There are basically two configurations of counterflow diffusion flames [2]: (1) a diffusion flame established between two opposed gaseous jets, one being fuel and the other being oxidant, and (2) a diffusion flame formed in the forward stagnation region of a porous spherical or cylindrical burner placed in a uniform oxidizer flow, with fuel being ejected uniformly from the burner surface. A counterflow diffusion flame can also be established when a condensed fuel is used, in which case the oxidizer flow is typically directed vertically downward toward the fuel surface with the flame forming at a distance above the fuel surface in the stagnation region. Alternatively, liquid fuel, which is fed to the porous burner surface at a rate equal to that of fuel consumption to ensure complete wetting of the surface and to prevent fuel dripping from the surface, is used to sustain a diffusion flame in the forward stagnation region of the burner. The counterflow geometry with a liquid spray has recently been used in the study of two-phase systems, such as droplet (Reference 3 and references therein).

Since a porous cylindrical burner (Tsuji burner) in a counterflow diffusion configuration has been extensively used to study flame structure [4,5,6] and flame extinction using inert gases [7], halons [8] and powders [8], it is logical to extend the application of such a burner configuration to other condensed-phase (e.g., aqueous or liquid) fire suppressants; therefore, a porous cylindrical burner was selected as a basis for the liquid agent screening apparatus.

Many advantages are associated with the use of a porous cylindrical burner in a counterflow diffusion configuration. The fuel and the oxidizer flows can be independently adjusted, if required. The flame is laminar, two-dimensional, and very stable in the forward stagnation region.

*This work is supported by DoD/NGP/SERDP.

The geometry of the burner and the flow field allow for relatively simple analysis of the forward stagnation region [9-15]. Both wake and enveloped flames can be easily maintained over a wide range of fuel and oxidizer flows. The flame is easily observed, and critical stages such as the blow-off limit (abrupt transition from an enveloped flame to a wake flame) can be ascertained with ease and high reproducibility. The flame front can be easily accessed by intrusive [5,6] or nonintrusive [10,15] probing techniques, thus enabling detailed studies of flame structure.

BURNER

The design of the burner is based on several important criteria. The burner has to be robust, easily built, installed, and operated, and able to generate reliable screen test data.

The burner is a **replaceable** porous ($20\ \mu\text{m}$) sintered stainless steel standard 0.5-in UNF threaded cup filter with a length of 3.18 cm (1.25 in), an i.d. of 1.12 cm (0.44 in), and an o.d. (D) of 1.58 cm (0.625 in). The advantage of this burner design over those used in the past is that burner replacement can be easily performed if partial or complete clogging of the porous burner surface occurs. The burner is screwed onto an extended insert through which fuel is injected into the interior of the porous filter and double-pass cooling water runs. The cooling water is used to cool the burner (to prevent damage to the porous surface structure) and the fuel (to prevent fuel pyrolysis prior to its ejection through the porous surface). A cross sectional schematic of the burner interior is shown in Figure 1.

The burner, together with the insert, does not completely span the entire test section of the wind tunnel. A cylindrical brass rod (same diameter as the burner) with internal water cooling is inserted from the opposite wall and is used as an extension so that the burner assembly (Figure 2) can be treated as a single cylinder across the test section. The rearward 180deg of the burner surface is coated with a thin layer of high-temperature resistant black paint in order to prevent fuel ejection into the wake region. The high-pressure drop across the porous sintered surface assures a very uniform fuel flow over the burner surface, thus the fuel ejection velocity (V_f) is calculated by dividing the fuel volumetric flow rate by the available fuel ejection area of the burner surface.

Propane is used as fuel; its flow rate is regulated by a mass-flow controller, which is controlled by a personal computer. A bubble flow meter was used to calibrate the mass-flow controller.

FLOW FACILITY

A small-scale vertically upward open-circuit wind tunnel is used to provide oxidizer (air) flow to the burner. The tunnel, except the test section, is made of clear polycarbonate (Lexan[®])* for visual observation of droplet transport toward the burner. The tunnel consists of a blower, a diffuser, a flow straightener, a contraction section, and a test section where the burner is placed in cross-flow. This configuration not only allows for the delivery of a uniform flow of oxidizer to

*Certain commercial products are identified in this paper to specify adequately the equipment used. Such identification does not imply recommendation by the National Institute of Standards and Technology, nor does it imply that this equipment is the best available for the purpose.

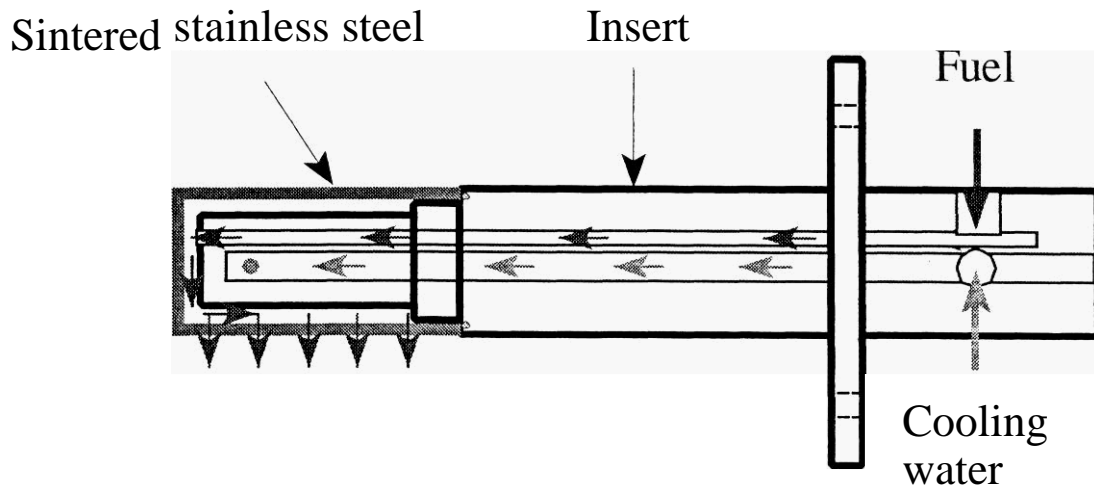


Figure 1. Cross sectional view of the burner.

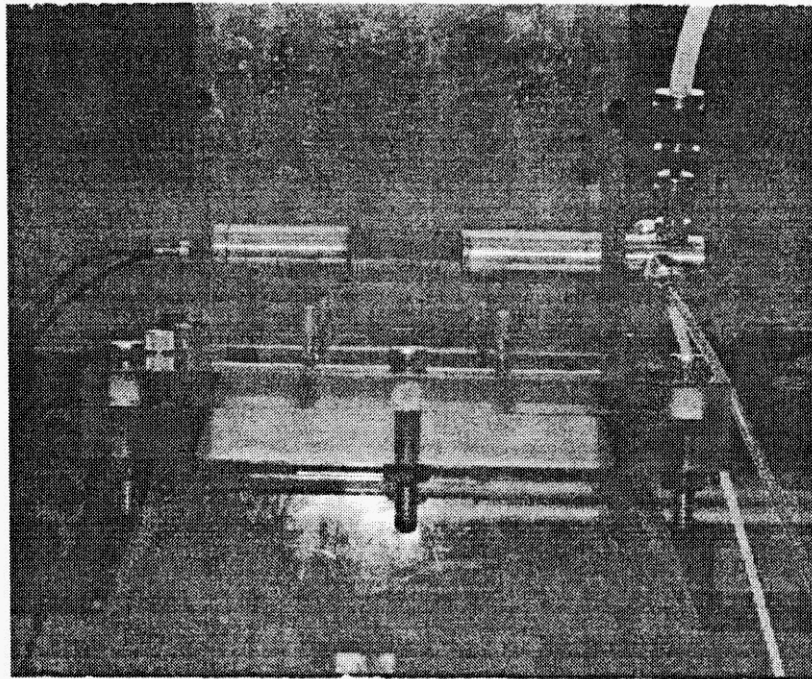
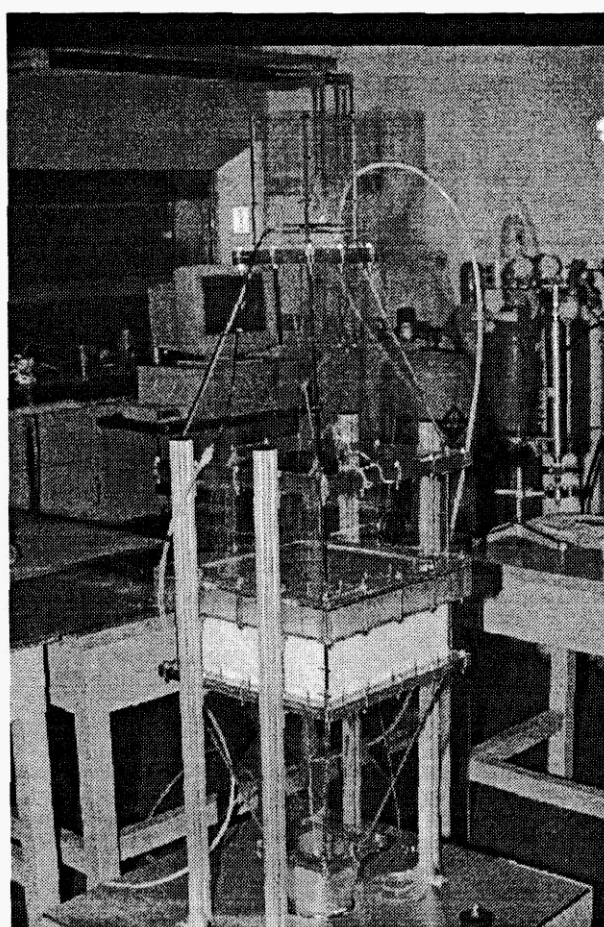


Figure 2. Photograph of the burner assembly.

the burner at a low turbulence intensity but also assists in the delivery of liquid agent droplets to the flame. Figure 3 is a photograph of the flow facility.

The air flow in the tunnel is provided by a variable-speed (frequency controlled) blower, whose outlet is connected to the main part of the wind tunnel via a flexible aluminum tube and a coupling to convert a circular cross section to a square. The blower was calibrated using a pitot probe equipped with a differential pressure transducer capable of measuring up to 1 torr. In the measurements, the Pitot-static tube was placed in the location where the burner would be mounted. The velocity profile obtained was relatively flat ($< \pm 0.5\%$) except in the region near the walls (boundary layers). Due to the limited frequency response of the pitot tube, the turbulent intensity level was not measured; however, the observation of a very stable laminar flame zone in the forward stagnation region of the burner provided a qualitative indication of low turbulent intensity. The volumetric flow rates are calculated using the measured average velocities (V_o) and the cross sectional area of the test section.



The diffuser with an inlet cross sectional area of 30 x 30 cm and an expansion ratio (based on areas) of 1:9 is 30 cm long. The flow straightener consists of a polycarbonate honeycomb with cell diameter of 0.32 cm (0.125 in) and a 50-mesh stainless steel screen with **30.3%** open area. The contraction section with a contraction ratio (based on areas) of 9: 1 has an inlet cross sectional area of 30 x 30 cm and is 30 cm long. A square flange, which was machined to have a smooth transition passage to minimize flow separation, is placed between the outlet of the contraction section and the inlet of the test section. The test section has a cross sectional area of

10 cm x 10 cm and a length of 20 cm. It is made of anodized aluminum with three Pyrex™ observation window (12 x 7 x 0.64 cm) flushly mounted on the three walls of the test section using high-temperature silicone RTV®. The burner is inserted through the fourth wall. The combustion products from the burner are vented to an exhaust hood.

DROPLET GENERATION

According to Rayleigh's analysis of the instability of capillary jets, the frequency f for maximum instability is given by the following equation [16]:

$$f = \frac{u_j}{4.508 d_j} \quad (1)$$

where u_j is the jet velocity and d_j is the jet diameter. When the jet is perturbed at this frequency, uniform sized droplets with uniform spacing are formed. Rayleigh's analysis is based on an inviscid liquid jet. Experimentally, mono-dispersed droplets can be generated within a range of frequencies [17]:

$$\frac{u_j}{7 d_j} < f < \frac{u_j}{3.5 d_j} \quad (2)$$

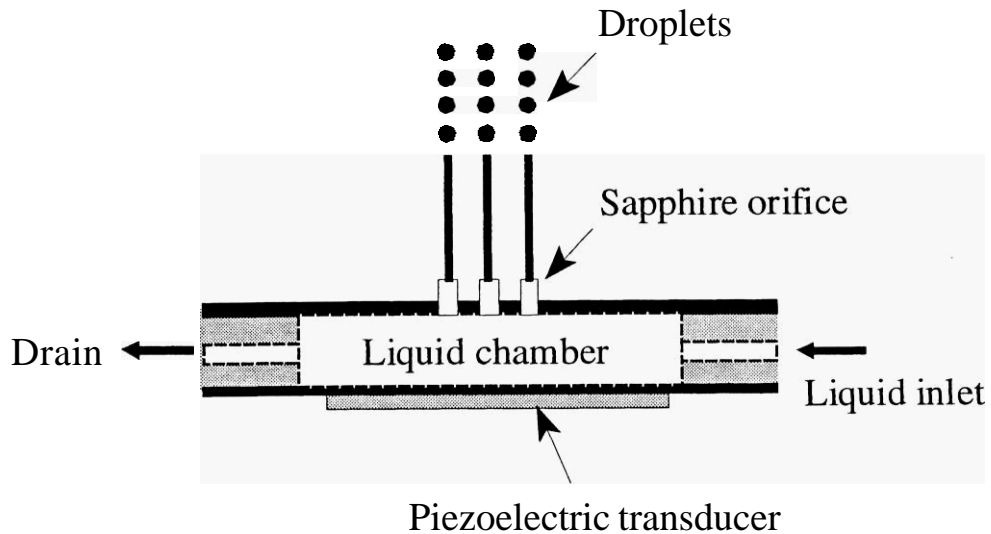
Depending on the droplet generator design, an extension of the above frequency range has been reported [18]. The droplet diameter, D , resulting from the controlled jet break-up can be calculated from the jet velocity and the imposed disturbance frequency using a simple mass balance, assuming the droplet mass is equivalent to that of a jet cylinder of length u_j / f and jet diameter d_j .

$$D = \left(\frac{6 Q}{\pi f} \right)^{1/3} \quad (3)$$

where Q is the volumetric flow rate of the jet. For a given flow rate, the droplet diameter can be varied by changing the perturbation frequency.

In our experimental apparatus, a piezoelectric droplet generator is used to create uniform liquid droplets ($< 250 \mu\text{m}$). The multiorifice piezoelectric droplet generator is similar to the design of Ashgriz and Yao [19]. The operating principle of the droplet generator is based on the break-up of multiple jets ejecting from a plate with multiple orifices as a result of controlled vibration from a piezoelectric transducer driven at a fixed frequency.

The droplet generator consists of a liquid chamber which is connected to a reservoir, a bleed port (for eliminating any air bubbles trapped inside the chamber during priming), an orifice plate, and a piezoelectric transducer. A schematic is shown in Figure 4. The initial jets emanating from the multi-orifice plate are obtained by pressurizing the liquid reservoir with nitrogen. Jetting from the orifice can be achieved with very low nitrogen pressurization ($\sim 0.03 \text{ MPa}$). A $0.5 \mu\text{m}$ filter is used in the liquid feedline to minimize clogging of the orifice openings due to potential foreign particulates in the liquid.



Several approaches for fabricating the orifice plate have been attempted, which include using sapphire orifices, laser drilled holes, and holes from photochemical machining (commercially available printhead). In our current setup, sapphire orifices are used because they are well fabricated to a tight tolerance, are not expensive, are readily available, and come in different size openings. Individual sapphire orifices are mounted on a set-screw, which can be easily attached to a plate to form a multiorifice plate. Our current generator has three orifice openings, which will provide sufficient flow to conduct the suppression experiments using liquid agents.

The droplet generator is located in the settling chamber and is approximately 42 cm upstream of the burner. The presence of the droplet generator in the wind tunnel does not create any significant perturbation or blockage effect on the oxidizer flow field near the burner because the flame characteristics do not change with or without the presence of the droplet generator in the flow stream. Although uniform size droplets with uniform spacing are observed several centimeters (~ 10 cm) from the orifices as a result of controlled jet break-up, the droplet behavior becomes random further downstream, which may be due to the wake and drag effects on the droplets in the stream. We are currently in the process of characterizing the droplet sizes and number densities at various locations near the burner forward stagnation point by using a Phase Doppler Particle Analyzer (PDPA). The uniformity of the droplet size will be assessed. Such information is needed to characterize the performance of the droplet generator before it can be successfully used for screening purposes.

CALIBRATION OF TEST FACILITY

The first step in calibrating the test facility was to ensure that the burner functioned properly. This was achieved by mapping out the flame stability diagram of the burner and by observing similar flame behavior to that described in References 4 and 5. There are two important parameters, fuel ejection velocity (V_f) and oxidizer velocity (V_o) in the wind tunnel, that govern the performance of the burner.

Under certain flow conditions, a thin, laminar, two-dimensional blue flame is established at a distance in front of the cylinder surface. An example is given in Figure 5(a). As the fuel ejection velocity is decreased or the air velocity is increased, the flame slowly approaches the cylinder surface, and eventually the flame is abruptly blown off from the stagnation region, and a wake flame, an example of which is shown in Figure 5(b), is established. Conversely, with increasing fuel velocity or decreasing air velocity, the flame zone gradually moves away from the surface of the cylinder, and eventually a laminar two-dimensional flame can no longer be sustained.

When the air velocity is very small and the fuel velocity is large, the flame zone becomes thicker, and an inner luminous yellow and an outer blue zones appear. When the air velocity is very large and reaches a critical value, the flame can never be stabilized, irrespective of the fuel ejection velocity.

Figure 6 shows the various flame stability regions of the burner obtained from the test facility. The abscissa is expressed as $2V_o/R$ (R being the burner radius) because this term represents the stagnation velocity gradient [4] and has the unit of strain rate (s^{-1}). Each data point in solid circle was obtained by increasing the fuel flow rate at a fixed oxidizer flow until a luminous yellow zone appeared. The conditions above these data points represent the existence of a yellow luminous zone. The data points in solid triangles represent the blow-off limit. Each data point was obtained by increasing the oxidizer flow at a fixed fuel ejection velocity until blow-off occurred. The conditions below the blow-off limit indicate the existence of a wake flame. However, the oxidizer flow will eventually reach a limiting or critical value as the fuel injection velocity increases. From Figure 6, this critical blow-off limit ($2V_o/R$), is $615 s^{-1}$. This value is similar to that obtained from Tsuji and Yamaoka [4,5] using a similar burner diameter. The region between these two data sets represents a stable enveloped blue flame stabilized at the forward stagnation region of the burner.

To evaluate its applicability to fire suppression screening of gaseous agents, the apparatus was also tested with propane and three inert gases: argon, helium, and nitrogen. At a predetermined air flow and a fixed fuel flow, the inert gas was metered into the oxidizer stream at the blower outlet via a dry-test meter and a metering valve. Extinction tests were performed by gradually adding the inert inhibitor to the oxidizer (air) stream until blow-off occurred (abrupt transition from enveloped to wake flame). The volumetric flow rates of inhibitor at blow-off were recorded. The experiments were then repeated with a different air flow.

Figure 7 shows the amount of nitrogen added as a function of $2V_o/R$ at blow-off at different fuel injection rates; V_o is the total volumetric flow rate of air and inert gas at blow-off. Each data point represents the average of at least two runs. The standard deviations are also plotted as error bars. Note that the scatter of the data also reflects date-to-date variations and the use of different replaceable burners. For a fixed $2V_o/R$, more nitrogen is needed to blow-off an enveloped flame as the fuel injection rate increases. For the same amount of nitrogen in the oxidizer stream, $2V_o/R$ at blow-off increases as the fuel injection rate increases.

The results for the three inert gases, argon, helium, and nitrogen, at one fuel injection rate are shown in Figure 8. For a given $2V_o/R$, argon requires the most amount added to the oxidizer stream to cause blow-off, whereas helium requires the least. The relative ranking of these three gases is comparable to those from cup-burner tests [1].

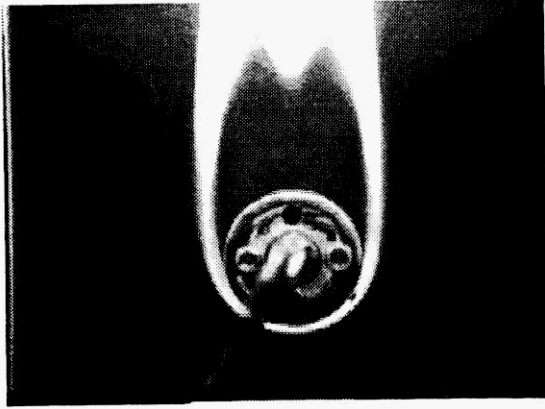


Figure 5(a). An enveloped flame.

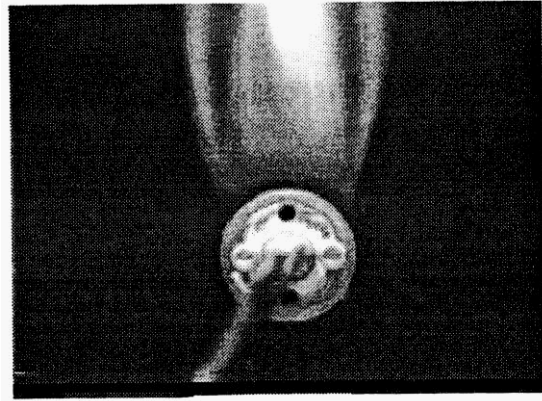


Figure 5(b). A wake flame.

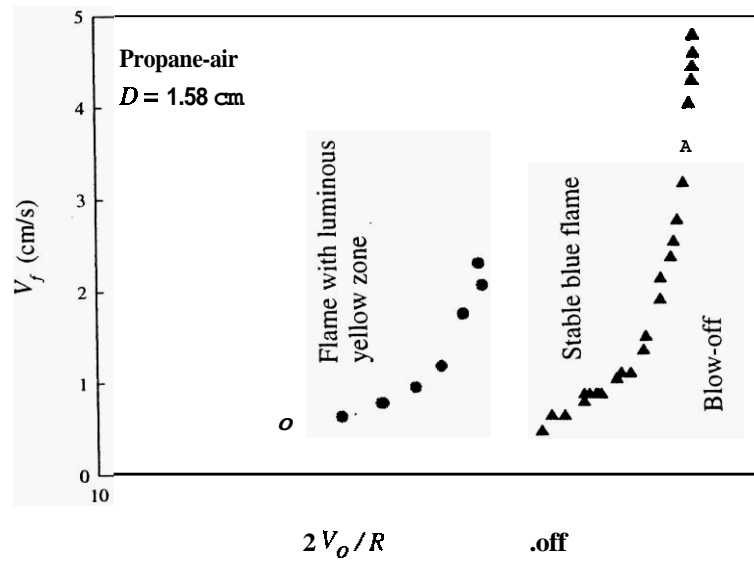


Figure 6. Flame stability diagram.

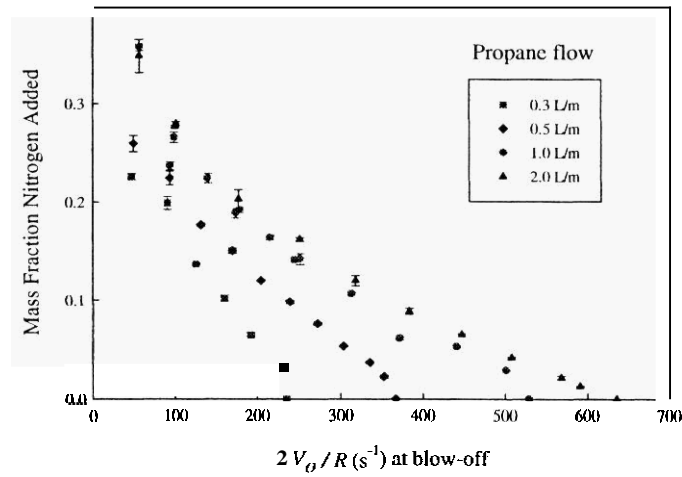


Figure 7. Mass fraction of nitrogen added in air as a function of stagnation velocity gradient at blow-off at different fuel flows.

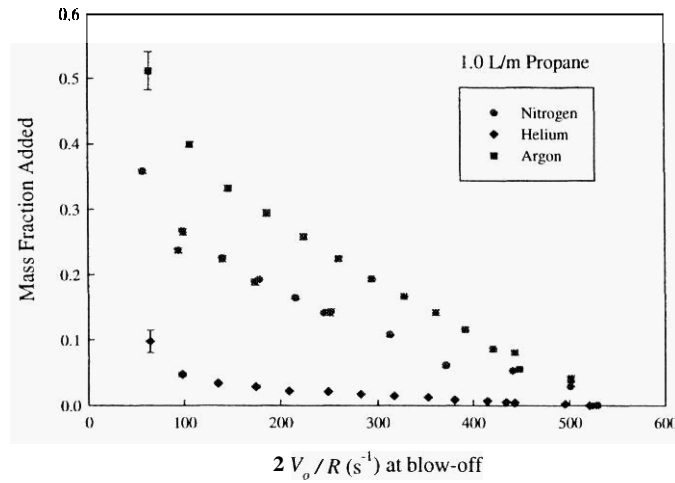


Figure 8. Mass fraction of various inert gases added in air as a function of stagnation velocity gradient at blow-off.

LIQUID SUPPRESSANT SCREENING

One of the most important steps in the liquid suppressant screening is to be able to deliver the liquid agent to the flame zone to cause suppression or extinction. A multiorifice droplet generator is used in the proposed screening in lieu of a spray because all the droplet streams, in principle, can be directed to the flame zone, thus minimizing droplet loss to the wall of the flow facility caused by the fan-out of a spray.

Preliminary tests using water droplets (without detailed droplet size measurements, yet) generated from one of the prototype generators have been performed. The experiments were conducted in the following manner. Upon the establishment of a stable enveloped flame at fixed fuel and oxidizer flows, droplet generation was initiated with a fixed water flow to the generator. The time interval between the arrival of the water droplets to the flame zone (which was indicated by an abrupt change in flame luminosity) and flame blow-off was noted from a CCD camera record. The time between the arrival of droplets at the flame zone and blow-off was found to increase with decreasing water flow at fixed fuel and oxidizer flows and to decrease with increasing oxidizer flow for a given fuel and water flows. The preliminary results are very promising and encouraging.

In our future tests, the following proposed experimental procedure will be adopted. At fixed fuel, oxidizer, and liquid flows, the time to reach blow-off is determined from a CCD camera record. At a fixed perturbation frequency and given orifice size, the droplets generated are expected to be mono-dispersed. The mass loading of the liquid to cause blow-off is then determined from the liquid mass flow and time to blow-off, assuming no droplet loss to the wind tunnel walls. The experiments are then repeated with a different air flow. A plot of mass loading at blow-off as a function of stagnation velocity gradient can then be constructed for various liquid agents to compare their suppression performances. Care should be exercised when higher oxidizer flow is used in the experiments because aerodynamic forces of the oxidizer may cause secondary disintegration of the liquid droplets; this will inadvertently make the interpretation of the suppression results less straightforward due to the introduction of droplet size effects. The maximum velocity that can be used to establish a stable enveloped flame for the experiments in our set-up is less than 2.5 m/s (based on the critical $2 V_o/R$ value of 615 s^{-1}); therefore, the aerodynamic effect on secondary droplet break-up is expected to be insignificant [16].

REFERENCES

1. Grosshandler, W.L., Gann, R.G., and Pitts, W.M., "Evaluation of Alternative In-Flight Fire Suppressants for Full-Scale Testing in Simulated Aircraft Engine Nacelles and Dry Bays," NIST SP861, U.S. Department of Commerce, April 1994.
2. Tsuji, H., "Counterflow Diffusion Flames," *Prog. Energy Combustion Sci.*, 8, 93 (1982).
3. Li, S.C., "Spray Stagnation Flames," *Prog. Energy Combustion Sci.*, 23, 303 (1997).
4. Tsuji, H. and Yamaoka, I., "The Counterflow Diffusion Flame in the Forward Stagnation Region of a Porous Cylinder," *Eleventh Symposium (International) on Combustion*, The Combustion Institute, Pittsburgh, PA, pp. 979-984, 1967.
5. Tsuji, H. and Yamaoka, I., "The Structure of Counterflow Diffusion Flames in the Forward Stagnation Region of a Porous Cylinder," *Twelfth Symposium (International) on Combustion*, The Combustion Institute, Pittsburgh, PA, pp. 997-1005, 1969.

6. Tsuji, H. and Yamaoka, I., "Structure Analysis of Counterflow Diffusion Flames in the Forward Stagnation Region of a Porous Cylinder," *Thirteenth Symposium (International) on Combustion*, The Combustion Institute, Pittsburgh, PA, pp. 723-731, 1971.
7. Ishizuka, S. and Tsuji, H., "An Experimental Study of Effect of Inert Gases on Extinction of Laminar Diffusion Flames," *Eighteenth Symposium (International) on Combustion*, The Combustion Institute, Pittsburgh, PA, pp. 695-703, 1981.
8. Milne, T.A., Green, C.L., and Benson, D.K., "The Use of the Counterflow Diffusion Flame in Studies of Inhibition Effectiveness of Gaseous and Powdered Agents," *Comb. Flame*, 15, 255 (1970).
9. Dixon-Lewis, G., David, T., Gaskell, P.H., Fukutani, S., Jinno, H., Miller, J.A., Kee, R.J., Smooke, M.D., Peters, N., Effelsberg, E., Warnatz, J., and Behrendt, F., "Calculation of the Structure and Extinction Limit of a Methane-Air Counterflow Diffusion Flame in the Forward Stagnation Region of a Porous Cylinder," *Twentieth Symposium (International) on Combustion*, The Combustion Institute, Pittsburgh, PA, pp. 1893-1904, 1984.
10. Dreier, T., Lange, B., Wolfrum, J., Zahn, M., Behrendt, F., and Warnatz, J., "CARS Measurements and Computations of the Structure of Laminar Stagnation-Point Methane-Air Counterflow Diffusion Flames," *Twenty-first Symposium (International) on Combustion*, The Combustion Institute, Pittsburgh, PA, pp. 1729-1736, 1986.
11. Peters, N. and Kee, R.J., "The Computation of Stretched Laminar Methane-Air Diffusion Flames Using a Reduced Four-Step Mechanism," *Comb. Flame*, 68, 17 (1987).
12. Olson, S.L. and T'ien, J.S., "A Theoretical Analysis of the Extinction Limits of a Methane-Air Opposed-Jet Diffusion Flame," *Comb. Flame*, 70, 161 (1987).
13. Dixon-Lewis, G. and Missaghi, M., "Structure and Extinction Limits of Counterflow Diffusion Flames of Hydrogen-Nitrogen Mixtures in Air," *Twenty-second Symposium (International) on Combustion*, The Combustion Institute, Pittsburgh, PA, pp. 1461-1470, 1988.
14. Chen, C.H. and Weng, F.B., "Flame Stabilization and Blowoff Over a Porous Cylinder," *Combust. Sci. Tech.*, 73, 427 (1990).
15. Sick, V., Arnold, A., Dießel, E., Dreier, T., Ketterle, W., Lange, B., Wolfrum, J., Thiele, K.U., Behrendt, F., and Warnatz, J., "Two-Dimensional Laser Diagnostics and Modeling of Counterflow Diffusion Flames," *Twenty-third Symposium (International) on Combustion*, The Combustion Institute, Pittsburgh, PA, pp. 495-501, 1990.
16. Bayvel, L. and Orzechowski, Z., *Liquid Atomization*, Taylor and Francis, Washington DC, 1993.
17. Schneider, J.M. and Hendricks, C.D., "Source of Uniform-Sized Liquid Droplets," *Rev. Sci. Instrum.*, 35, 1349 (1964).
18. Warnica, W.D., Van Reenen, M., Renksizbulut, M., and Strong, A.B., "A Piezoelectric Droplet Generator for Use in Wind Tunnels," *Rev. Sci. Instrum.*, 62, 3037 (1991).
19. Ashgriz, N. and Yao, S.C., "Development of a Controlled Spray Generator," *Rev. Sci. Instrum.*, 58, 1291 (1987).